An Alternative to the Quark-Gluon Structure of the Proton

William L. Stubbs*

No Affiliation, 1961 SW Davis Street, Port Saint Lucie, FL 34953

Drafted 29 October 2015

Abstract

I explore the question: Does the deep inelastic scattering data support a simpler, more accommodating, model of the proton than the quark-gluon model?; and present a case for an alternative to the current proton model. By reanalyzing the SLAC proton and deuteron F_2 curves, I show that the proton can be modeled as nine muons. Then, by reevaluating the F_2 results of the HERA proton deep inelastic scattering experiments, I further show that the muons in this proton model are each made of just over 200 electrons. A model of the free electron falls out of the new proton model that reveals why the Bohr magneton only approximates the free electron magnetic moment, and that the mass of the electron neutrino is 236 eV. Finally, by slightly modifying my proton model, I build a model of the neutron that reveals 0.24 MeV of energy not currently accounted for in the neutron mass-energy balances used to determine its mass. From all of this, I conclude that the deep inelastic scattering data does support a simpler, more accommodating, model of the proton than the quark-gluon model, and question the validity of the quark model.

Keywords: proton; deep inelastic scattering; quark; gluon

* *E-mail address*: ift22c@bellsouth.net

1. Introduction

Nowadays, everyone knows that the proton is made of three particles called valance quarks, an abundance of quark-antiquark pairs called sea quarks, and a mass of chargeless particles called gluons [1]. The model originates from the deep inelastic scattering experiments done at the Stanford Linear Accelerator Center (SLAC) in the late 1960s and early 1970s [2,3,4,5,6], and was reinforced by experiments performed at the Hadron Electron Ring Accelerator (HERA) in the 1990s [7]. The SLAC experiments established that the proton contains charged, [8] spin-½, [9] particles. These attributes aligned it with a theory of elementary particles proposed by Gell-Mann [10], and independently by Zweig, [11] in 1964. Among other things, the theory posited that the proton is made of three particles Gell-Mann labeled quarks. Initially, Gell-Mann's quarks were not well received in the high-energy physics community [12]. They had, at least, two problems.

First, Gell-Mann's quarks had fractional charges. In his theory, the proton's charge comes from two up quarks, each with a $+{}^{2}/_{3}$ charge, and one down quark, with a charge of $-{}^{1}/_{3}$. No particles having fractional charges had ever been observed in nature. Second, prior to the SLAC experiments, most people considered the proton a fundamental particle. Almost no one thought that the proton was made of particles. Consequently, no one thought Gell-Mann's quarks were real. They were considered "mathematical constructs" [1,12]. However, the discovery of particles inside the proton eliminated the second problem. This swayed the opinions of Gell-Mann's peers. By 1969, the high-energy physics community had embraced the quarks [1] and focused its efforts on validating that, indeed, they were the particles discovered inside the proton [1,13]. However, the experimental results did not completely support the three-quark proton model.

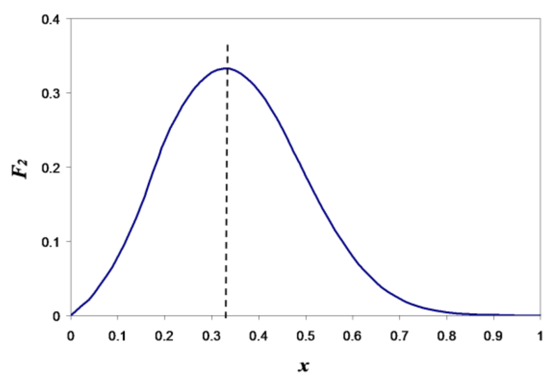

Figure 1: The shape of an F_2 curve for a proton made of just three quarks.

According to the parton model [14,15,16], the particles inside the proton produce a structure function distribution, F_2, that is a function of the fraction of proton momentum, x, the particles carry. The F_2 structure function characterizes the momentum distribution of the particles inside the proton. A proton made of just three quarks would have an F_2 curve that looks something like the curve in Figure 1. It would rise from about $F_2 = 0$ at $x = 0$, to some peak value at about $x = {}^{1}/_{3}$, then gradually fall back to zero near $x = 1$ [16].

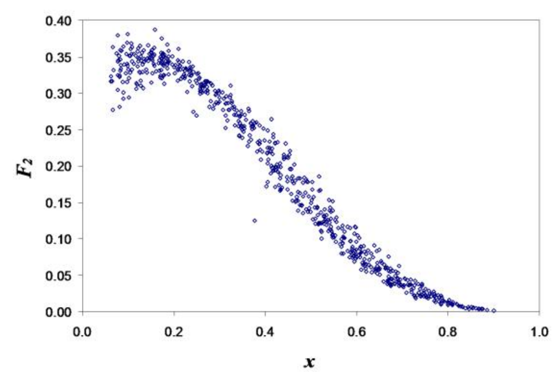

Figure 2: The SLAC proton F_2 structure function values for fraction of proton momentum, x.

However, the SLAC proton F_2 curve showed no peak. Figure 2 shows the SLAC proton F_2 curve. It was interpreted to be flat at a value of roughly 0.34 from $x = 0.08$ to $x = 0.20$, then to decline to 0 at about $x = 0.90$. There was no data available for $x < 0.08$, but given the behavior from $0.08 < x < 0.20$, the thinking was that F_2 was probably 0.34 or higher starting from $x = 0$.

To explain this behavior in terms of quarks as proton constituents, SLAC attributed the high F_2 values for $x < {}^1/_3$ to particles eventually called sea quarks, a collection of quark-antiquark pairs. These sea quarks are radiated by the three, so-called, valence quarks, the three quarks originally thought to form the proton. [15,16]. SLAC used exercises involving neutron scattering cross sections as a basis for this claim.

SLAC measured scattering cross sections for the proton and the deuteron [6], but could not directly measure neutron cross sections because the neutron is unstable. Since the deuteron is a proton bound to a neutron, Bodek subtracted proton cross sections from deuteron cross sections to extract neutron scattering cross sections [17]. He examined the neutron-over-proton cross section ratios as a function of x and found that for low-x values, as $x \rightarrow 0$, the ratio approached 1. F_2 was thought to be dominated by sea quark in the low-x region, and this ratio of 1 indicated their dominance and showed the neutron and the proton had the equal amounts of them [17].

Bodek also used the neutron cross sections to generate neutron F_2 values [17], and subtracted the neutron F_2 values from the proton F_2 values. Since the proton and the neutron were thought to contain about the same amount of sea quarks; subtracting the F_2 values of one from the other would remove them from the difference. The result would show the F_2 behavior of only the three valence quarks.

The result of the subtraction was an F_2 curve of the difference between the proton and the neutron F_2 curves that peaked at $x = 0.35$. This was close enough to $x = {}^1/_3$ to declare that the results revealed evidence of the three valence quarks. Because they were revealed as a result of the subtraction, it appeared the exercise also verified the existence of the sea quarks in the proton. However, even with the sea quarks in the proton model, it remained inadequate. Calculations showed that the valence quarks together with the sea quarks only accounted for 54% of the proton's momentum [16]. There appeared to be something else inside the proton.

Finally, to supplement the momentum shortfall of the quarks, the chargeless particles called gluons were introduced into the proton model [16,18]. Since gluons have no electric charge, the thinking was that they are there, but the electrons probing the proton in deep inelastic scattering cannot see them. The "phantom" gluons were assigned the missing proton momentum, and the proton model became the quark-gluon model that it is today. Not quite the model Gell-Mann proposed in 1964. Its complexity begs the question: Does the deep inelastic scattering data support a simpler, more accommodating, model of the proton than the quark-gluon model?

Here, I explore that question and present a case for an alternative to the quark-gluon proton model. By reanalyzing the SLAC proton and deuteron F_2 curves, I will show that the proton can also be modeled as nine particles. Then, by reevaluating the F_2 results from the HERA proton deep inelastic scattering experiments, I will further show that the nine particles making up this alternative proton model are, in turn, each made of just over 200 particles. I will show that a model of the electron falls out of the new proton model that reveals why the Bohr magneton only approximates the electron magnetic moment, and offers a value for the electron neutrino mass. Finally, I will show that by slightly modifying my proton model, I get a neutron model that reveals some energy not accounted for in mass-energy balances used to determine its mass.

I organized this paper as follows. First, I review the SLAC deep inelastic scattering results. Then, I analyze the F_2 structure function results to determine the number and types of particles in the proton. Next, I review the early HERA deep inelastic scattering results. I analysis the F_2 structure function from those results to determine the structure they reveal within the proton. Using the findings of the aforementioned analyses, I then propose new models of the muon, proton, electron and neutron. Finally, I close with some conclusions drawn from my analyses.

2. SLAC Deep Inelastic Scattering Experiments

I began by reassessing the electron-proton (*e-p*) and electron-deuteron (*e-d*) deep inelastic scattering data from the original SLAC experiments that were interpreted to show a three-quark proton structure. I analyzed the structure function curves for both the proton and deuteron to determine the behavior of the data. In doing so, I sought to determine, without bias from existing interpretations, what the data revealed about the number and types of particles inside the proton.

2.1 Brief Review of SLAC Results

SLAC measured the inelastic scattering cross sections for *e-p* and *e-d* collisions at laboratory scattering angles, θ, ranging from 6º to 34º [2]. The electrons carried an initial energy, E, between 4.6 and 30 GeV, and scattered off the targets with energy, E', between 1 and 10 GeV. Reference [19] gives the complete list of angles, energies, cross sections and structure functions collected from the experiments. The structure function F_2, was calculated using the QED expression for the differential scattering cross section [6]

$$\frac{d^2\sigma}{\partial\Omega\partial E'}(E, E', \theta) = \sigma_{Mott}\left[W_2(\nu, Q^2) + 2W_1(\nu, Q^2)\tan^2\left(\frac{\theta}{2}\right)\right], \tag{1}$$

where

$$\sigma_{Mott} = \frac{4\alpha^2 E'^2}{Q^4}\cos^2\left(\frac{\theta}{2}\right) \text{ is the Mott cross section,} \tag{2}$$

α = the fine structure constant,

W_1 and W_2 are structure functions,

$$\nu = E - E' \text{ is the energy transferred to the proton by the virtual photon, and} \tag{3}$$

$$Q^2 = 4EE'\sin^2\left(\frac{\theta}{2}\right) \text{ is the invariant 4-momentum transfer.} \tag{4}$$

Bodek [6] showed that the structure function $W_2(\nu, Q^2)$ can be expressed as

$$W_2(\nu, Q^2) = \frac{1}{\sigma_{Mott}}\frac{d^2\sigma}{\partial\Omega\partial E'}\left[1 + \left(\frac{2}{1+R(\nu, Q^2)}\right)\left(\frac{Q^2+\nu^2}{Q^2}\right)\tan^2\left(\frac{\theta}{2}\right)\right]^{-1}, \tag{5}$$

where

$R(\nu, Q^2) = \sigma_L/\sigma_T$,

σ_L is the longitudinal virtual photon absorption cross section, and

σ_T is the transverse virtual photon absorption cross section.

The two photon absorption cross sections can be extracted from experimental data collected [19] and used to produce $R(\nu, Q^2)$. The structure function $W_2(\nu, Q^2)$ can then be calculated using the $R(\nu, Q^2)$ values. Whitlow *et al.* determined [20] the $R(\nu, Q^2)$ values for the SLAC experiments discussed here. Bjorken showed [8] that in the limits of $\nu \to \infty$ and $Q^2 \to \infty$, W_2 became the function of a single dimensionless variable x,

$$\nu W_2(\nu, Q^2) \rightarrow F_2(x) \tag{6}$$

where

$$x = \frac{Q^2}{2M\nu} \ . \tag{7}$$

This new F_2 structure function depends only on the fraction of the proton's momentum, x, carried by the particle inside the proton struck by the electron. Whitlow *et al.* produced the SLAC proton and deuteron F_2 structure functions values discussed here, which are listed in [19]. Figure 3 and Figure 4 show graphs of the SLAC F_2 data as a function of the fraction of proton momentum the struck particles struck carry, x, for the proton and the deuteron, respectively.

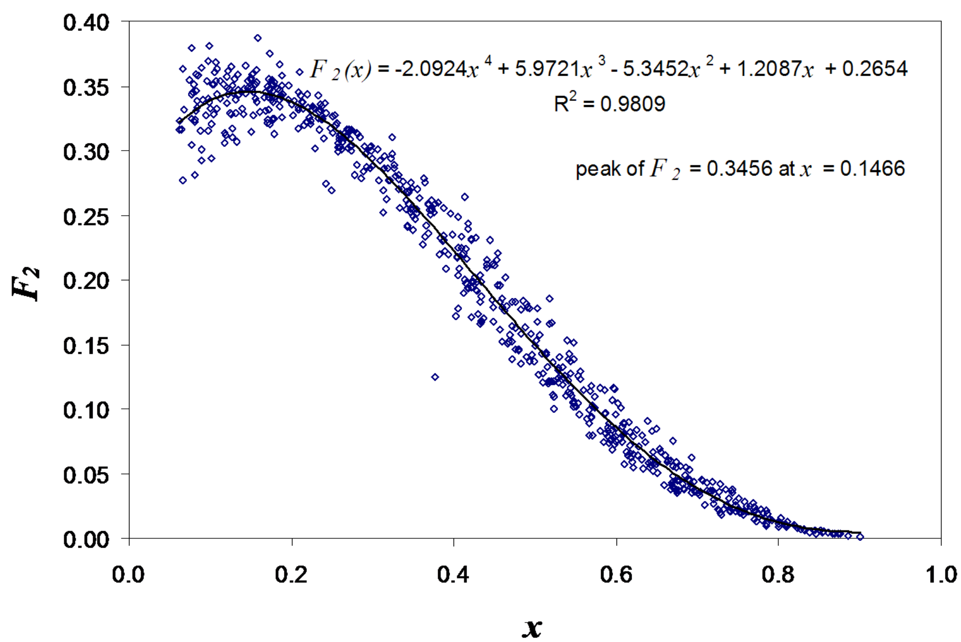

Figure 3: The SLAC proton F_2 structure function values plotted as a function of the fraction of proton momentum x. A least-squares polynomial fit of the points is included. The peak F_2 value and its corresponding momentum fraction according to the fit are also given.

2.2 SLAC Structure Function Analysis

The F_2 structure function gives insight into the momentum distribution of the particles inside the deep inelastic scattering target. If the particles all have the same mass, then the F_2 curve peaks at the target momentum fraction corresponding to the reciprocal of the number of particles in the target [16]. A target made of n particles produces an F_2 curve that peaks at $x = {}^1/_n$. This means that the F_2 curve of a target made of three particles would peak at about $x = {}^1/_3$.

The SLAC proton F_2 curve (Figure 3) is well behaved and very easy to analyze. In order to get a better sense of where the scattering of points in the curve peaks, I fitted them with a very good ($R^2 = 0.980$) fourth-order least-squares polynomial. The equation of the fit is

$$F_2\,(x) = -\,2.0924x^4 + 5.9721x^3 - 5.3452x^2 + 1.2087x + 0.2654. \tag{8}$$

The fit curve drawn through the points clearly showed that an F_2 maximum occurs at some x value less than $x = 0.2$. I set the derivative of the F_2 equation equal to zero, solved for the momentum fraction, x, and found that the curve peaked at $x = 0.1466$. The reciprocal of this value is 6.82. This indicated that the proton is made of in the neighborhood of seven particles.

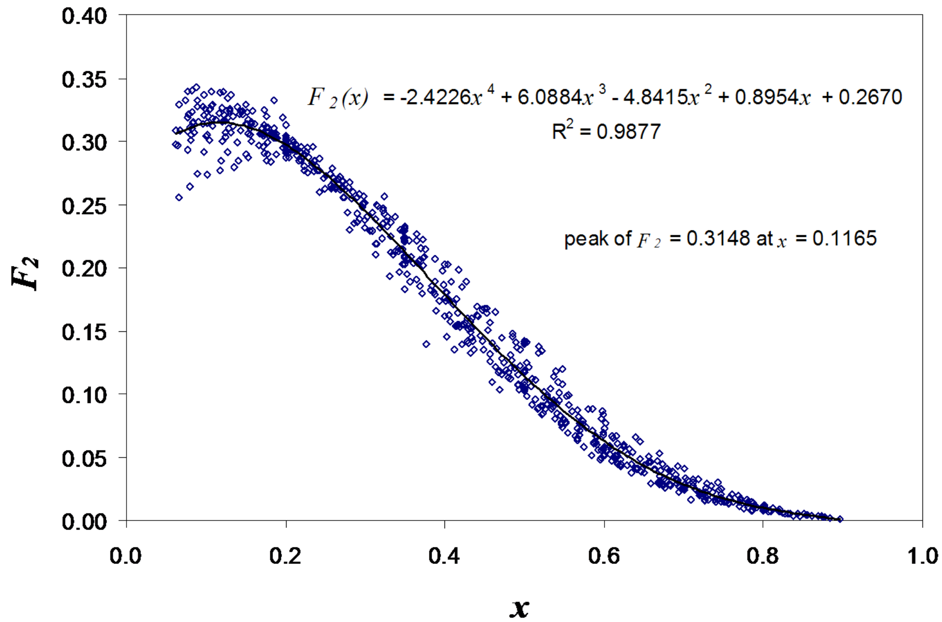

Figure 4: The per-nucleon SLAC deuteron F_2 structure function values plotted as a function of the fraction of proton momentum, x. The actual F_2 values are twice that shown on the graph. A least-squares polynomial fit of the points is included. The peak F_2 value and its corresponding momentum fraction according to the fit are also given.

The structure function data for the deuteron substantiated the implication of the proton curve. The deuteron F_2 curve in Figure 4 is a per-nucleon curve. This means that it represents what an individual nucleon in the deuteron looks like, not the whole deuteron. My fourth-order polynomial fit through the deuteron points gave the F_2 equation

$$F_2\,(x) = -\,2.4226x^4 + 6.0884x^3 - 4.8415x^2 + 0.8954x + 0.2670. \quad (9)$$

Again, the data is well behaved (fit $R^2 = 0.988$). The fit showed a peak F_2 at $x = 0.1165$. The reciprocal of this momentum fraction is 8.58. Therefore, the deuteron data implies that the two nucleons in the deuteron are each made of nine particles. So, the proton and deuteron F_2 data indicated that the proton and the neutron are made of seven to nine particles, not three.

I noticed that the momentum fractions on the deuteron graph in Figure 4 are the momentum fractions of a proton, not a deuteron. When I inspected the SLAC data [19], I found that for runs with identical E, E' and Q^2 values, the calculated x values for the proton and the deuteron are the same. This means that the mass value used by SLAC to calculate x for the deuteron was the proton mass (see equation (7)), not the target deuteron mass. Figure 5 shows what the deuteron F_2 curve looks like when its x-axis reflects the momentum fraction of the deuteron. In it, I replaced the proton x values originally paired with the F_2 values, with x values I calculated using the deuteron mass of 1.876 GeV instead of the proton mass of 0.938 GeV. In the figure, I also restored the F_2 values to their true deuteron values by multiplying the reported values by 2.

Figure 5 shows that the deuteron F_2 structure function curve actually peaks at deuteron momentum fraction $x = 0.0583$. The reciprocal of this momentum fraction is 17.15. Since this value is greater than 17, it means that there are more than 17 particles in the deuteron. Given the per-nucleon indication of nine particles per nucleon, I interpreted the deuteron F_2 curve to show that the deuteron contains 18 particles.

The figure also shows that the true deuteron F_2 structure function curve goes to zero at about $x = 0.5$ instead of $x = 1$, as it did when the x-axis reflected the proton momentum fractions. This is significant because it indicates that the particles struck during the scattering can only carry a maximum of half of the deuteron's momentum. That means that they are confined to only one of the nucleons in the deuteron, so each nucleon is made of nine particles.

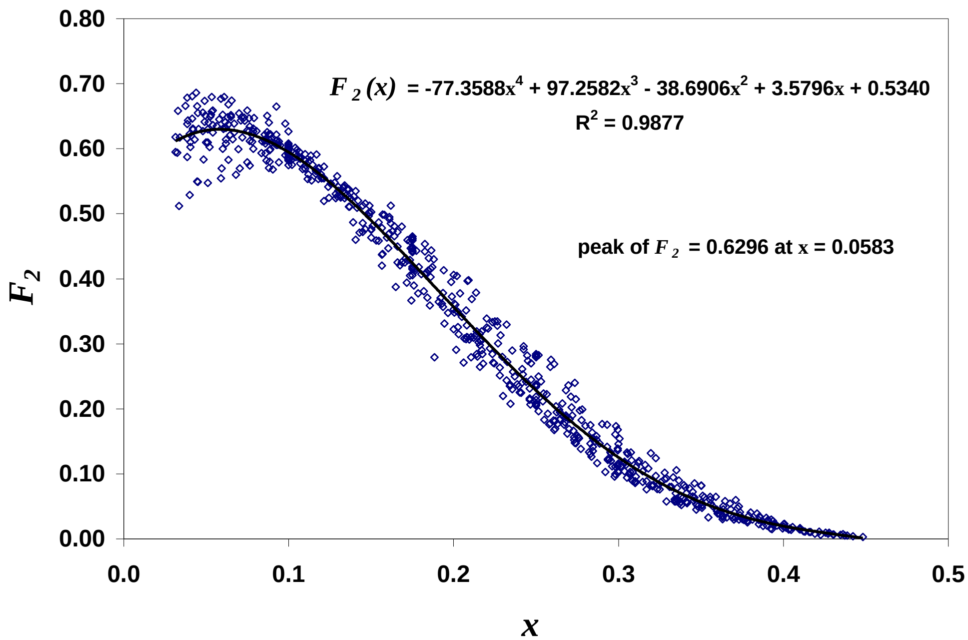

Figure 5: The true SLAC deuteron F_2 structure function values plotted as a function of the fraction of deuteron momentum, x. A least-squares polynomial fit of the points is included. The peak F_2 value and its corresponding momentum fraction according to the fit are also given.

2.3 Proton Constituent Particles

Based on my reanalysis of the SLAC deep inelastic scattering data for the proton and the deuteron, I concluded that the proton and the neutron are each made of nine particles. The deuteron F_2 structure function curve indicated that the deuteron is made of 18 particles, two nucleons that each contains nine particles. The question then became: What are the particles? I knew that these particles are charged particles, and that they are spin ½ particles. I assumed that, since there are nine of them in a proton, the mass of these particles is about $^1/_9$ that of the proton. I found that the known particle that came closest to meeting all of these criteria was the muon.

The muon and its antiparticle, the antimuon, are spin ½ particles that carry a charge, $q = -1$ for the muon and $q = +1$ for the antimuon. The mass of a free muon is 105.658 MeV, which makes the proton 8.88 times as massive as it. Free muons are short-lived particles, having a mean lifetime of about 2.2 microseconds. However, confinement within a proton may extend the muon's lifetime somehow, just as confinement within a nucleus does for the neutron.

2.4 Analysis Validation

A series of *e-p* and *e-d* deep inelastic scattering experiments (E99-118) were done at the Thomas Jefferson National Accelerator Facility (JLAB) in 2000 [21]. They appear to validate my contention that the high proton F_2 values measured by SLAC for $x < {}^1/_3$ do not indicate the existence of sea quarks in protons, just more than three particles. JLAB generated F_2 structure function data for momentum fractions, x, between 0.009 and 0.45, and momentum transfers, Q^2, between 0.06 GeV^2 and 2.8 GeV^2. The data extends the SLAC F_2 structure functions shown in Figure 3 and Figure 4 back from roughly $x = 0.09$, down to $x = 0.009$, using scattering electrons with momentum transfers comparable to those used at SLAC. This captures a picture of that region of the proton F_2 curve at a resolution similar to that used to generate the SLAC curves.

Figure 6 and Figure 7 show the SLAC proton and deuteron F_2 structure function data from Figure 3 and Figure 4 with the JLAB data added. Table 1 shows the JLAB data used. It was taken directly from Table II of Reference [21]. The figures show that the F_2 values of the proton and nucleons of the deuteron drop off steeply to near zero as their momentum fractions approach $x = 0$ from $x \sim 0.09$. This behavior of the F_2 structure function in this region of the momentum fraction is consistent with the behavior predicted by Figure 1, but with a nine-particle proton, not three. The proton and the deuteron graphs show clearly, without curve fits, that their F_2 values peak in the vicinity of $x = 0.11$ or $x = {}^1/_9$. The JLAB F_2 values at $x = 0.45$ and $x = 0.25$ (circled) show that JLAB data integrates well with the original SLAC F_2 data.

Table 1
F_2 structure function values for the proton (F_2 - p) and the deuteron (F_2 - d) as a function of x and Q^2 from the JLAB E99-118 deep inelastic scattering experiments [21]

x	Q^2	F_2 - p	F_2 - d	x	Q^2	F_2 - p	F_2 - d
0.009	0.034	0.056	0.0492	0.04	0.287	0.2027	0.2002
0.009	0.051	0.0616	0.058	0.04	0.353	0.2244	0.2077
0.009	0.086	0.0997	0.0896	0.04	0.37	0.2288	0.2139
0.015	0.059	0.0696	0.0669	0.04	0.371	0.2186	0.2155
0.015	0.095	0.0842	0.0831	0.04	0.38	0.2102	0.2231
0.015	0.098	0.0961	0.0935	0.04	0.421	0.2416	0.2268
0.015	0.112	0.0876	0.0966	0.06	0.18	0.1641	0.1616
0.015	0.127	0.1058	0.1073	0.06	0.479	0.2622	0.2563
0.015	0.144	0.1114	0.1129	0.06	0.491	0.2617	0.2702
0.015	0.151	0.1216	0.1186	0.06	0.543	0.2751	0.2609
0.015	0.164	0.1253	0.1227	0.06	0.633	0.2863	0.2958
0.015	0.172	0.1118	0.1286	0.08	0.456	0.265	0.2451
0.025	0.067	0.0883	0.0834	0.08	0.617	0.2935	0.2752
0.025	0.092	0.096	0.0953	0.08	0.619	0.296	0.2767
0.025	0.104	0.104	0.0994	0.08	0.799	0.3128	0.295
0.025	0.113	0.1069	0.1024	0.08	0.818	0.3227	0.3122
0.025	0.14	0.1251	0.1208	0.125	0.588	0.2876	0.2609
0.025	0.186	0.1469	0.1441	0.125	0.797	0.3179	0.2873
0.025	0.195	0.1312	0.1439	0.125	1.032	0.3319	0.2952
0.025	0.212	0.1675	0.1545	0.125	1.056	0.3491	0.3228
0.025	0.222	0.1593	0.1568	0.175	1.029	0.3242	0.2846
0.025	0.24	0.178	0.1656	0.175	1.045	0.3235	0.2939
0.025	0.252	0.1696	0.1745	0.175	1.365	0.3447	0.3072
0.025	0.253	0.153	0.1601	0.25	1.332	0.3126	0.2673
0.025	0.287	0.1669	0.1814	0.25	1.761	0.3183	0.2744
0.04	0.133	0.1295	0.128	0.45	2.275	0.2104	0.1638
0.04	0.273	0.2038	0.1876				

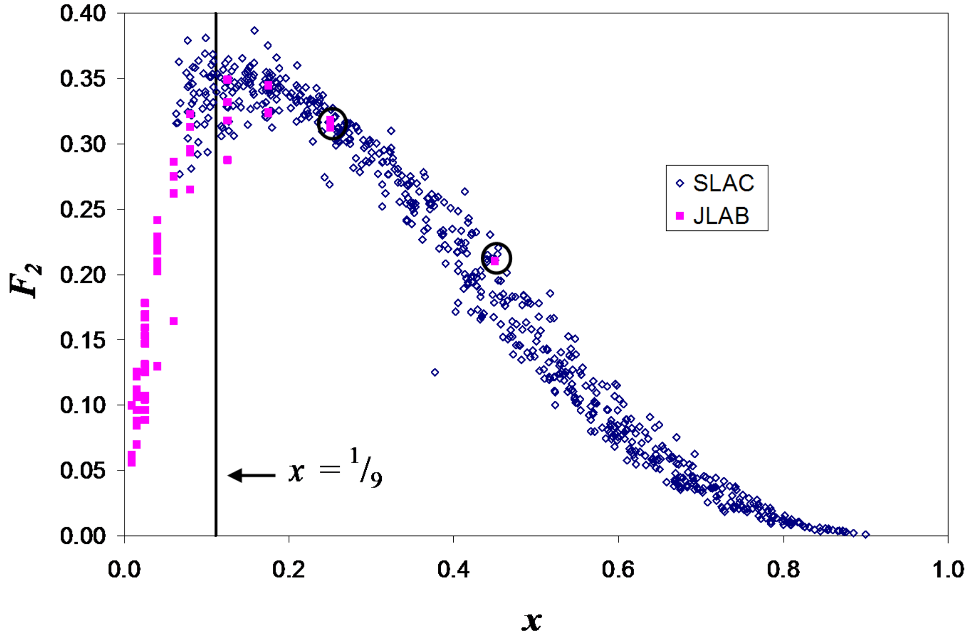

Figure 6: SLAC proton F_2 curve with low-x, low-Q^2 data from JLAB appended.

The complete F_2 structure function curves for the proton and the deuteron show that the F_2 values for $x < {}^1/_3$ are not inflated due to the electrons scattering off sea quarks. Instead, the F_2 values are rising as $x \rightarrow 0$ from $x = {}^1/_3$, to a peak that occurs at $x = {}^1/_9$, before falling back down to near zero as x goes to zero. This clearly indicates that the proton is made of nine particles, not the three quarks posited by Gell-Mann. This low-x, low-Q^2 structure function data shows that the sea quarks claimed to be seen in the SLAC experiments, were not really there.

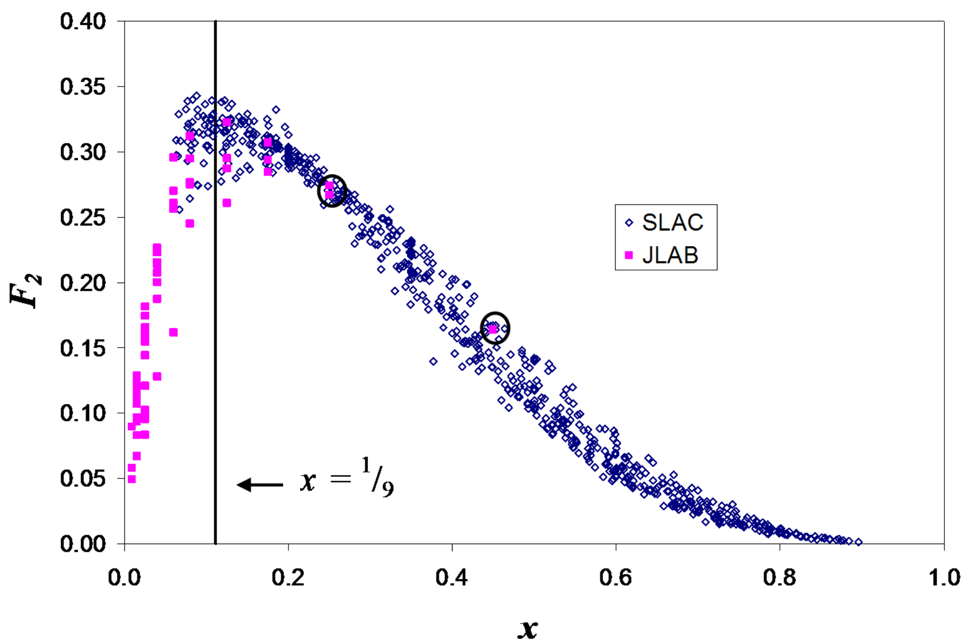

Figure 7: SLAC deuteron F_2 curve with low-x, low-Q^2 data from JLAB appended.

3. HERA Deep Inelastic Scattering Experiments

Once I identified the muon as the proton constituent particle, it became clear that the high F_2 structure function values at low momentum fractions for the proton no longer needed to be interpreted as the sea quarks. The nine muons carried all of the proton's momentum. However, I also knew that extensive work had been done in the low-x region at HERA. Therefore, I decided to reanalyze some of the original HERA *e-p* deep inelastic scattering data. This data was low-x data, interpreted as the electrons scattering off the sea quarks and antiquarks [22].

3.1 Brief Review of HERA Experimental Results

The data I used was from a set of experiments performed in 1993 [7]. These experiments measured electron-proton scattering cross sections for momentum fractions from x = 0.133, which is in the neighborhood of the SLAC curve peak value, down to x = 0.000178. The momentum transfers, Q^2, ranged from 4.5 GeV^2 for very low x values, up to 1,600 GeV^2 for the higher x values. Table 2 gives the F_2 structure function values determined for the specified momentum fraction, x, and momentum transfer, Q^2.

Table 2
F_2 structure function values as a function of x and Q^2 from the HERA 1993 proton deep inelastic scattering experiments [7]

x	Q^2 (GeV^2)															
	4.5	6	8.5	12	15	20	25	35	50	65	80	120	200	400	800	1600
0.000178	1.16	1.21	1.19													
0.000261			1.20	1.35												
0.000383			1.11	1.26	1.40											
0.000562				1.19	1.35	1.52										
0.000825				1.08	1.17	1.17	1.71									
0.00133				0.96	1.13	1.03	1.23	1.23	1.46							
0.00237				0.85	0.94	1.03	1.02	1.10	1.08	1.40	1.09	1.60				
0.00421				0.74	0.78	0.83	0.91	0.97	1.00	1.09	1.19	0.99	1.41			
0.00750				0.70	0.71	0.74	0.73	0.88	0.65	0.95	0.70	0.83	0.91	1.16		
0.0133				0.58	0.59	0.64	0.71	0.86	0.66	0.69	0.71	0.73	0.72	0.81	1.13	
0.0237						0.51	0.52	0.57	0.52	0.50	0.60	0.65	0.54	0.71	0.82	
0.0421								0.55	0.40	0.48	0.47	0.34	0.37	0.78	0.67	0.86
0.075											0.45	0.48		0.42	0.57	0.62
0.133														0.31	0.30	0.37

Relative to the SLAC structure function data, the HERA data shown in Table 2 is low-x, high-Q^2 data. The electron scattering done at HERA was typically much higher energy scattering than that done at SLAC. Most of the scatterings done at SLAC with momentum fractions of $x < 0.17$ were done at momentum transfers of $Q^2 < 2.0$ GeV^2, and many of them with $Q^2 < 1.0$ GeV^2. Table 2 shows that the lowest Q^2 used for the HERA data was $Q^2 = 4.5$ GeV^2, and only for one point. None of the SLAC F_2 values with momentum fractions of $x < 0.17$ had momentum transfers as high as $Q^2 = 4.5$ GeV^2.

Similarly, the JLAB scatterings were done at very low energies compared to the HERA events. All of the JLAB F_2 values for momentum fractions of $x < 0.1$ had momentum transfers of $Q^2 < 1.0$ GeV^2. The maximum momentum transfer in the JLAB scattering experiments was $Q^2 = 2.275$ GeV^2, only about half the lowest HERA value.

Consequently, HERA was seeing a much different picture in this low-x region than SLAC or JLAB was seeing. The difference was probably analogous to that of a microscope (HERA) versus a magnifying glass (SLAC/JLAB).

3.2 HERA Structure Function Analysis

After reviewing the HERA proton F_2 structure function values shown in Table 2, I realized that they were a continuation of the SLAC proton structure examination with a higher resolution probe. I noticed that at $x = 0.13$, scaling was still in play. The HERA F_2 values of 0.31, 0.30 and 0.37 for Q^2 equal to 400 GeV^2, 800 GeV^2 and 1,600 GeV^2, respectively, were comparable to the SLAC F_2 values of 0.30 to 0.36, for momentum fractions in that neighborhood at much lower Q^2 values. However, when the momentum fraction drops to around $x = 0.075$, the SLAC data, with Q^2 between 1 GeV^2 and 2 GeV^2, was still showing F_2 values in the neighborhood of 0.30, while the HERA F_2 values had climbed to a range of 0.45 to 0.62 for Q^2 from 80 GeV^2 to 1,600 GeV^2.

I recognized this as a transition that occurs in the HERA deep inelastic scattering data between $x = 0.075$ and $x = 0.13$, which includes the momentum fraction $^1/_9$ that the muons within the proton carry. I realized that when the energies of the probing electrons were very high, producing very short electron wavelengths, the electrons ceased probing the proton, and began probing the muons within the proton.

To show that the transition from probing the proton to probing the muon had occurred, I converted the proton F_2 data to data for the muon. First, I adjusted the HERA proton F_2 values in Table 1 to muon F_2 values by subtracting the SLAC proton F_2 value corresponding to the peak momentum fraction, $F_2 = 0.3456$, from them. This set the muon F_2 value to approximately zero for the proton momentum fraction of $^1/_9$, which corresponds to a muon momentum fraction of 1.

Next, I adjusted the momentum fractions in the HERA data from proton momentum fractions to muon momentum fractions since the electron target is now the muon. I did this by replacing the proton mass with the mass of the muon in the expression for x given in equation (7). Since the muon's mass is $^1/_9$ the proton's mass, to adjust to the muon momentum fractions, I simply multiplied the proton momentum fractions by 9.

Finally, I averaged the HERA F_2 values for a given momentum fraction to produce a single F_2 value for each x value. Table 3 shows the averaged values for the original proton data and the adjusted data, which is the muon data.

Table 3
The original (proton) and adjusted (muon) F_2 structure function data from the 1993 HERA proton deep inelastic scattering experiments averaged for momentum fraction x. The adjusted x values are the original values multiplied by 9 to convert them to muon momentum fractions. The adjusted F_2 values are the original values minus 0.3456 to convert them to muon F_2 structure function values.

Index	Original (Proton) Data		Adjusted (Muon) Data	
No.	x	F_2	x	F_2
1	0.000178	1.187	0.001602	0.841
2	0.000261	1.275	0.002349	0.929
3	0.000383	1.257	0.003447	0.911
4	0.000562	1.353	0.005058	1.007
5	0.000825	1.320	0.007425	0.974
6	0.001330	1.173	0.011970	0.827
7	0.002370	1.123	0.021330	0.777
8	0.004210	0.991	0.037890	0.645
9	0.007500	0.815	0.067500	0.469
10	0.013300	0.736	0.119700	0.390
11	0.023700	0.594	0.213300	0.248
12	0.042100	0.565	0.378900	0.219
13	0.075000	0.508	0.675000	0.162
14	0.133000	0.327	1.197000	-0.019

I plotted the adjusted F_2 values from Table 3 in Figure 8. This is the F_2 structure function curve for the muon. I excluded two points from the graph, $x = 0.003447$ and $x = 1.197$. I noticed that the F_2 value for $x = 0.003447$ trends counter to the values around it. As x increases in this region, so does the corresponding F_2. However, the F_2 value for $x = 0.003447$ decreased. I felt this strongly suggested that the F_2 value may be bad and omitted it. I also recognized that a momentum fraction of 1.197 is more momentum than a particle within the muon can carry. Therefore, it is outside the scope of the muon's structure function curve and was also omitted.

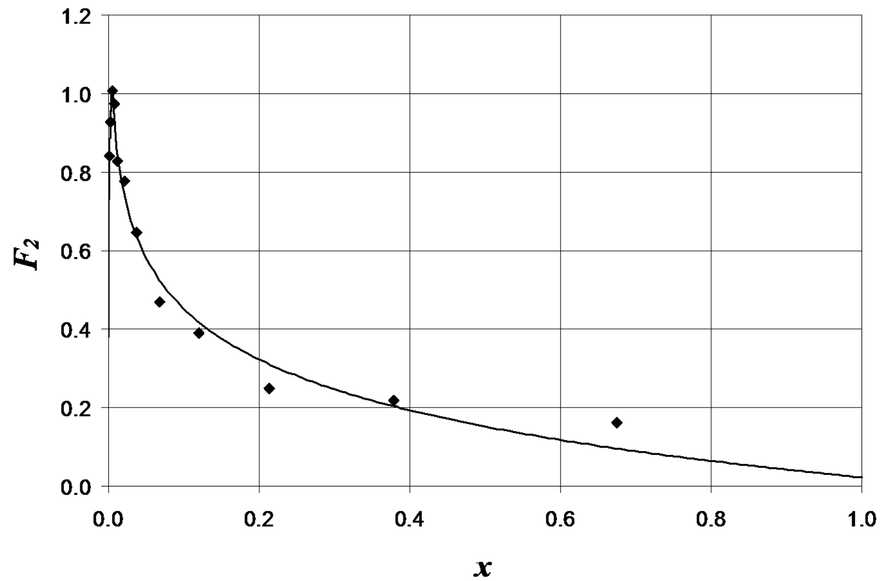

Figure 8: The HERA muon F_2 structure function values (Table 3) plotted as a function of the fraction of muon momentum, x. Two least-squares logarithmic curve fits are drawn through the points.

The curve rises up to a sharp peak of $F_2 \sim 1$ for a momentum fraction of about $x = 0.005$. The peak at this momentum fraction indicates that the muon is made of in the neighborhood of 200 particles. The sharp peak F_2 value of approximately 1 indicates that these particles do not interact strongly with each other. I took this to means that they probably do not bind to each other as the muons in the proton appear to do.

Figure 9 zooms in on the portion of the curve in Figure 8 containing the peak F_2 value. I broke the F_2 curve in this graph into two parts to fit it. The first fit curve covers the three points $x = 0.001602$, $x = 0.002349$, and $x = 0.005058$. This covers the climb of the F_2 values from zero up to the vicinity of the peak. I used a logarithmic fit that tracked the points with the equation

$$F_2(x) = 0.1388 \text{ Ln}(x) + 1.7483. \tag{10}$$

The second fit curve starts at $x = 0.005058$ and covers the 10 points out to $x = 0.675$. It takes the F_2 values from the peak through the descent down to values approaching zero at $x = 1$. I also used a logarithmic for it. The fit equation is

$$F_2(x) = -\,0.1866 \text{ Ln}(x) + 0.0220. \tag{11}$$

I determined the momentum fraction that corresponded to the peak F_2 structure function value for the muon by setting fit equation (10) equal to fit equation (11) and solving for the momentum fraction, x. The result indicated that a peak F_2 structure function value of 1.0119 occurs at momentum fraction $x = 0.004966$. This would make the muon be about 201 particles.

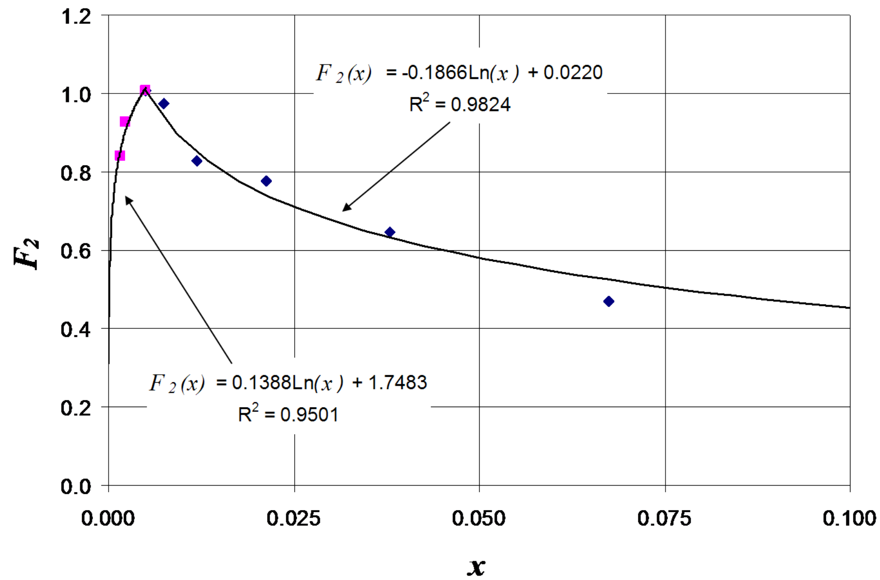

Figure 9: The HERA muon F_2 structure function values (Table 3) plotted as a function of the fraction of muon momentum, x, through $x = 0.1$. Two least-squares logarithmic curve fits are drawn through the points.

When the deep inelastic scattering target is made of a collection of particles that do not interact with each other, its F_2 structure function curve is a δ-function. The F_2 value is 1 at the momentum fraction equal to the reciprocal of the number of particles in the target, and zero everywhere else [16]. Interaction between the particles causes the F_2 curve to spread out and the peak F_2 value to fall below 1. My muon F_2 curve is not a δ-function, but Figure 8 shows that it has a sharp narrow peak that approximates the δ-function. Therefore, ideally, the F_2 value should reach a peak just short of 1 at the x value corresponding to the reciprocal of the number of particles forming the muon. However, the peak F_2 value of the two fit curves slightly overshoots 1. I suspected this near miss was probably due to the data used to produce the two curve fits.

I expected the two fit curves to meet at just under $F_2 = 1$, forming a peak at the actual momentum fraction the component particles carry. However, the two curves pass through $F_2 = 1$ rather than meet just short of there. This is likely due to uncertainties in my curve fits because of the small sample size of data used to produce them. The curves miss the mark.

I suspected that the two curves should meet at no greater than $F_2 = 1$, but that one curve's prediction of the momentum fraction that gives $F_2 = 1$ was low, and the other curve's prediction was high. This caused them to meet at $F_2 > 1$. I compensated for this by using as the actual peak momentum fraction, the x value midway between the two x values that make the F_2 values of the two curve fits equal 1. The x value that makes $F_2 = 1$ in fit equation (10) is $x = 0.004556$. The x value that makes $F_2 = 1$ in fit equation (11) is $x = 0.005294$. The x value that lies midway between these two solutions is the momentum fraction $x = 0.004925$. This value of x became my momentum fraction value for where the muon structure function peaks.

3.3 Muon Constituent Particles

With the value x = 0.004925 as the momentum fraction where the peak F_2 value occurs for the muon, the reciprocal of 0.004925, or 203, should be the number of particles inside the muon. This indicates that the muons inside a proton are made of about 203 particles. A free muon has a mass that is 206.77 times the mass of an electron. Since electrons are charged, spin ½, particles, I concluded that the particles inside the muon were most likely electrons. A free muon must be made of 207 electrons to match its mass.

4. Particle Models

Using the results from the reanalysis of the SLAC and the HERA deep inelastic scattering data, I developed new models of the muon, proton, electron and neutron.

4.1 Muon Model

I was able to use the results from the analysis of the HERA electron-proton deep inelastic scattering data to show that a free muon is made of 207 electrons. When I say the muon is made of electrons, I really mean electrons and positrons. The muon and antimuon are charged particles. The only way I can produce their charges is by using combinations of electrons, possessing a unit negative charge, and positrons, having a unit positive charge. Since the muon has a charge of -1, and the antimuon a charge of +1, the muon must contain one more electron than positron, and the antimuon, one more positron than electron. This means that, to be made of 207 particles, the muon must contain 103 positrons and 104 electrons, and the antimuon must contain 104 positrons and 103 electrons.

My analysis showed that the muons and antimuons inside the proton have less than 207 particles. The proton's mass is 1,836.15 times that of an electron. If the muons and antimuons that form the proton are made exclusively of electrons and positrons, then the proton is made of only electrons and positrons. To cover its mass, the proton must be made of 1,837 electrons and positrons. This means that the nine muons and antimuons are each made of about 204 electrons and positrons. Since, to produce their charges, muons need one more electron than positron and antimuons need one more positron than electron, both are made of an odd number of particles. Therefore, they are made of either 203 or 205 particles. In order to produce the proton's 1,837 particles, four of its muons must be made of 203 particles, and five of them, 205 particles.

The muon model I propose here appears to support the observed decay of the muon. Free muons decay in microseconds into an electron, a muon neutrino and an electron antineutrino,

$$\begin{aligned} \mu^- &\rightarrow e^- + \nu_\mu + \bar{\nu}_e, \\ \mu^+ &\rightarrow e^+ + \bar{\nu}_\mu + \nu_e. \end{aligned} \tag{12}$$

The two neutrinos are virtually massless. Therefore, during the decay, essentially all of the muon's mass but one electron converts to energy. If the free muon is the collection of 104 electrons and 103 positrons described above; then, it appears once free, 103 of its electrons and 103 of its positrons almost instantly annihilate each other. This leaves the lone unpaired electron as its massive decay product. The same thing occurs in the decay of the antimuon except its 103 annihilations leave a lone positron as its decay product.

The sharp narrow peak of the muon F_2 structure function curve and its peak F_2 value of nearly 1 indicate that the electrons and positrons in the muon do not interact strongly with each other. I took this to mean that they do not bind to each other. Instead, they only influence each other via their electric fields. The positively charged positrons attract the negatively charged electrons and repel other positrons; and the negatively charged electrons attract the positrons and repel other electrons. I suspect that a balance of these forces within the muons inside the proton somehow keeps the particles separated from each other. However, once the muon is outside the proton, the balance breaks down and the muon collapses. This causes the electron-positron annihilations within the muon to occur that causes its decay.

4.2 Proton Model

I now offer an alternative to the current model of the proton. Recall, the current proton model is made of two up quarks and one down quark called valence quarks, none of which have been directly observed in nature. It has an undetermined number of quark-antiquark pairs called sea quarks that have never been observed in nature, and an undetermined number of particles called gluons, also never observed in nature. My alternative proton model is made of muons and antimuons, particles routinely observed in nature.

My proton is made of four muons and five antimuons in order to produce the protons +1 charge. The proton and deuteron F_2 curves indicate that the particles inside the proton interact with each other. I modeled this interaction as binding. As a result, the muons inside my proton display a mass defect similar to that protons and neutrons show within the nucleus. The muons forming the proton are slightly less massive than a free muon.

Free muons and antimuons are made of 207 particles, but the four muons inside a proton are made of 203 particles and the five antimuons, 205 particles. The muons inside the proton are made of 102 electrons and 101 positrons, and the antimuons inside the proton are made of 102 electrons and 103 positrons. This gives my proton model 918 electrons and 919 positrons, or 1,837 electron-sized particles. They cover the proton's mass of 1,836.15 electron masses.

In my proton model, the confined muons and antimuons compensate for their particle deficiencies by sharing electrons and positrons with each other. They share electrons and positrons with each other in order to configure themselves with a full compliment of 207 particles. By sharing the particles, they also bond to each other.

Figure 10 shows an example of how this bonding works. In the example, a muon bonds to two antimuons by sharing four of its particles, an electron-positron pair with each antimuon. The electron-positron pair each antimuon receives from the muon added to its 205 particles gives it a total of 207 particles, making it equivalent to a free antimuon. In return, each antimuon shares two of its particles, an electron-positron pair, with the muon. Having the two additional electron-positron pairs raises the muon's particle number by four, from 203 to 207, making it equivalent to a free muon. Because the particles they share are now a part of both the muon and the antimuon, the two are melded together. The muon needs the particles from the antimuons to be whole and the antimuons need the muon's particles to be whole, so they must stay together.

This type of bonding holds the muons and antimuons together in my model to form the proton. They share whatever number of particles they need to all have 207. Particle sharing between muons and antimuons of different nucleons is likely what also binds nucleons together to form the nucleus of the atom. This would mean that there is no strong force, and that the nucleus the atom is just a collection of muons and antimuons sharing electrons and positrons.

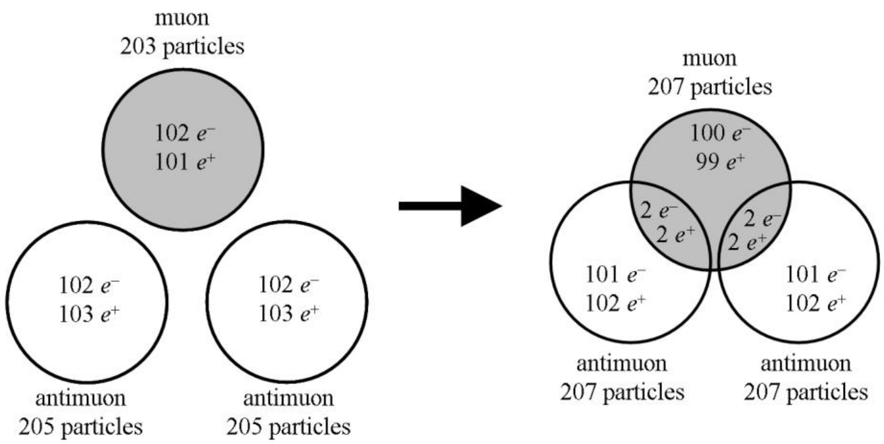

Figure 10: Example of how two antimuons might bond with a muon inside the proton by sharing electrons and positrons. Each antimuon shares one of its positrons and electrons with the muon and the muon shares one of its positrons and electrons with each antimuon. Through sharing particles, both antimuons and the muon have the 207 particles of free antimuons and muons.

I suspect that the proton peak structure function value of $F_2 \sim {}^1/_3$ indicates that the muons and antimuons within the proton form three-particle clusters, or trimuons. In turn, the trimuons bond to each other to form a configuration like that shown in Figure 11. However, at this time I have no analytical or experimental basis for this claim. The diagrams in Figure 11 just show what I think the inside of the proton looks like.

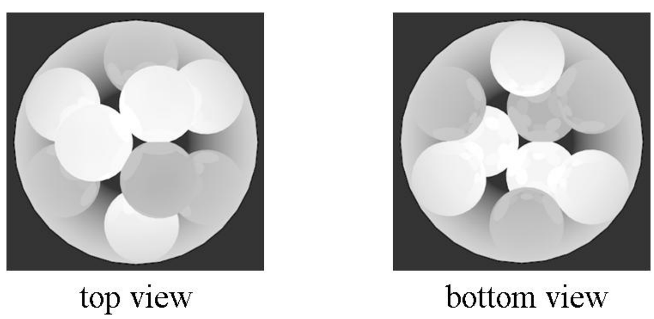

Figure 11: Two views of the suspected configuration of the muons (shaded) and antimuons (white) within the proton. The muons and antimuons form trimuons. Two trimuons are formed by two antimuons and a muon bonding, and one trimuon is an antimuon and two muons bound together. The three trimuons bond to each other.

Observations of muons and antimuons in nature support a proton made of the particles. Muons and antimuons seem to appear whenever protons are shattered. Cosmic rays consist primarily of high-energy protons [23]. Muons are produced when they collide with molecules in the Earth's atmosphere. Protons made of muons and antimuons would explain the source of the muons produced by cosmic rays. Muons and antimuons also appear during the electron-proton deep inelastic scattering experiments as muon-antimuon pairs [24]. Again, if protons are made of muons and antimuons, these pairs are likely fragments of the proton shattered by the scattering event. These occurrences strongly support a proton made of muons and antimuons.

4.3 Electron Model

From my proton model, I was able to develop a model of the electron. The proton mass is 1,836.15 times the electron mass, but my proton model contains 1,837 electrons and positrons. Similarly, the mass of the muon is 206.77 times the mass of an electron, but its model is 207 electrons and positrons. They seem minor, even negligible; but I assumed these discrepancies were significant. They suggested that the electrons and positrons inside the muon, and consequently, the proton, are slightly less massive than free electrons and free positrons.

The 1,837 electrons and positrons inside my proton only equaled the mass of 1,836.15 free electrons and positrons. That meant the mass of an electron inside the proton appeared to be 0.99954 times the mass of a free electron. The fact that electrons and positrons inside the muon also appeared to be less massive than free electrons and positrons (0.99889) indicated that the difference between the two kinds of electrons was probably real. Since the proton is a stable particle, but the muon is not, I chose the proton mass to use as the standard mass and established that confined electrons in my proton model are 0.99954 times as massive as free electrons.

I modeled the difference between an electron inside a proton and a free electron by making the free electron a composite particle made of the electron found inside the proton and a neutrino. I set the mass difference between the free and confined electrons as the mass of the neutrino. Since the mass of the confined electron is 0.99954 times the mass of a free electron, and the only difference in the particles is the neutrino, then the mass of the neutrino is 0.00046 electron masses, or about 236 eV. This is about 100 times greater than the ~2.5 eV currently considered the upper mass limit of an electron neutrino [25,26], but about 700 times less than the 170 keV mass limit of the muon neutrino [27]. Therefore, 236 eV is not an unreasonable mass for a neutrino.

I can interpret electron capture as a physical demonstration that the free electron carries a neutrino with it, but electrons inside the proton (nucleus) do not. When an orbital electron is pulled into the nucleus during electron capture, a neutrino is observed as a byproduct of the process. For example,

$$ {}^{11}_{6}C + {}^{0}_{-1}e \rightarrow {}^{11}_{5}B + \nu_e . \tag{13}$$

If the electrons inside the nucleus do not carry neutrinos, but free electrons do; then I submit that the neutrino appears during the process because the nucleus will not accept the companion neutrino of the free electron it captures.

Call the electrons inside the nucleus (and the proton) “beta” electrons. Then, the free electron appears to be a beta electron coupled with a neutrino. Electron capture produces essentially the same outcome as positive beta decay. It removes a positron from the nucleus. Therefore, the free electron drawn in by the nucleus must annihilate one of the positrons in the nucleus. When this happens, it leaves a free neutrino within the nucleus. The nucleus apparently ejects the neutrino, and the capture process is complete.

Conversely, when the nucleus emits a beta particle (beta positron or beta electron), a neutrino or an antineutrino is the decay product of beta decay. For example,

$$ {}^{3}_{1}H \rightarrow {}^{3}_{2}He + {}^{0}_{-1}e + \bar{\nu}_e , \tag{14}$$

$$ {}^{13}_{7}N \rightarrow {}^{13}_{6}C + {}^{0}_{+1}e + \nu_e . \tag{15}$$

In these cases, the beta particle captures an antineutrino to become a free positron or a neutrino to become a free electron.

The beta particle leaves the nucleus. However, I submit that, to exist as a free particle outside the nucleus, it must have a companion neutrino. Therefore, I propose that the decay produces a 472 eV photon (γ) that splits into a neutrino and an antineutrino by pair production. A beta electron captures the neutrino to become a free electron, and the antineutrino flies off as a decay product. A beta positron captures the antineutrino to become a free positron, and the neutrino becomes a decay product. Now equations (14) and (15) become

$$\begin{aligned} {}^{3}_{1}H &\rightarrow {}^{3}_{2}He + \beta^{-} + \gamma \\ &\rightarrow {}^{3}_{2}He + \beta^{-} + (\nu_e + \bar{\nu}_e) \\ &\rightarrow {}^{3}_{2}He + (\beta^{-} + \nu_e) + \bar{\nu}_e \\ &\rightarrow {}^{3}_{2}He + {}^{0}_{-1}e + \bar{\nu}_e \,, \end{aligned} \tag{16}$$

$$\begin{aligned} {}^{13}_{7}N &\rightarrow {}^{13}_{6}C + \beta^{+} + \gamma \\ &\rightarrow {}^{13}_{6}C + \beta^{+} + (\bar{\nu}_e + \nu_e) \\ &\rightarrow {}^{13}_{6}C + (\beta^{+} + \bar{\nu}_e) + \nu_e \\ &\rightarrow {}^{13}_{6}C + {}^{0}_{+1}e + \nu_e \,. \end{aligned} \tag{17}$$

At this time I cannot explain how a beta electron and a neutrino couple together to form a free electron. However, I suspect that the beta electron somehow encapsulates the neutrino in order to keep it from escaping the configuration. I can interpret the electron magnetic moment in a way that appears to support this notion. At first glance, it seems that the electron magnetic moment, μ_e, should be equal to the Bohr magneton, μ_B, but it is not. The electron magnetic moment is 1.00116 times the Bohr magneton [28]. The difference is small, but there is a difference, and the question becomes: What is causing it?

I noticed that the dimensions of the magnetic moment – usually expressed as Joules per Tesla (J/T) – reduce down to Coulombs meters-squared per second (C-m^2/s). This makes the magnetic moment look like the product of a “moment of charge” (C-m^2) and a frequency (s^{-1}), with the moment of charge that I speak of being the charge-equivalent of the moment of inertia for mass (kg-m^2). Therefore, I could express the magnetic moment μ of a charged particle as $\mu = I_q \nu$, where I_q is the moment of charge of the particle and ν is its rotating frequency. This meant that, since the moment of inertia (mass) for a solid sphere is $I = {}^2\!/_5\, mr^2$ and for a thin-shelled hollow sphere, $I = {}^2\!/_3\, mr^2$; the moment of charge for a solid sphere would be $I = {}^2\!/_5\, qr^2$, and for a thin-shelled hollow sphere, $I = {}^2\!/_3\, qr^2$, where m and q are mass and charge, respectively.

In the case of the electron, its (classical) radius is roughly three times that of the proton, but its mass is 1,836 times smaller than the proton’s mass. Assuming the density of particle matter is constant, the electron appears to be a thin-shelled hollow particle. This makes the electron’s moment of charge $I_e = {}^2\!/_3\, q_e\, r_e^2$. The Bohr magneton, $\mu_B = -\ 9.27401\ x\ 10^{-24}$ J/T, approximates the electron magnetic moment, $\mu_e = -\ 9.28476\ x\ 10^{-24}$ J/T, with $\mu_e = 1.00116\ \mu_B$. Since the electron’s magnetic moment is slightly larger than the Bohr magneton, I reasoned that; if the electron were actually a small charged particle in a high-speed orbit about some central entity, the precession of its orbital plane about an axis of revolution through the central entity would make the electron appear to be a thin-shelled hollow sphere. This is why the Bohr magneton so nearly matches the electron's magnetic moment. The moment of charge of a thin-shelled hollow sphere approximates the moment of charge of the electron's orbiting particle. However, it is not exactly the electron's moment of charge.

Figure 12 is a diagram of the model I am proposing. The small circle is the charged particle (what I now call a beta electron) orbiting the neutrino located at the center of the orbit. The large circle is the orbit of the beta electron and the vertical line dissecting the large circle is the axis about which the orbital plane is spinning. The electron appears to spin about this axis, so I calculated its moment of charge with respect to this axis.

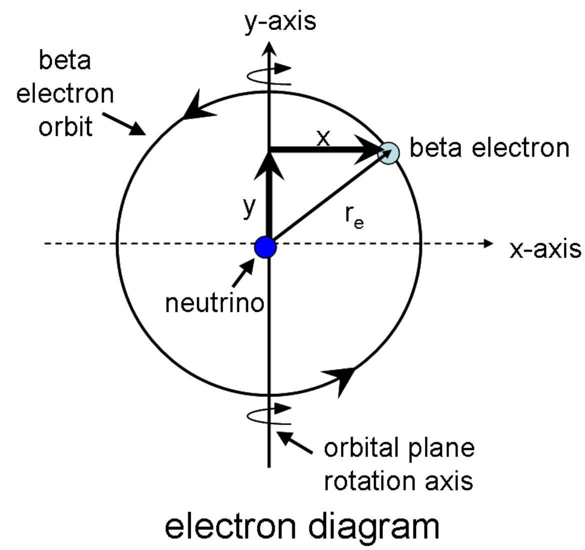

Figure 12: A diagram of the electron depicted as a beta electron orbiting a neutrino. As the beta electron orbits, the orbit rotates about the y-axis creating the illusion of a hollow sphere.

The electron's moment of charge has two components in this configuration. Because the orbit of the particle spins on an axis, I had to calculate the moment of charge using the parallel axis theorem [29]. Briefly, the parallel axis theorem states that the moment of inertia of a body with respect to an axis not through the body, I', is equal the moment of inertia of the body, plus the product of the mass of the body and the average distance squared the body is from the desired axis, or $I' = I + md^2$, where d^2 is the average distance squared from the axis. Paralleling this concept to the moment of charge gives $I' = I + qd^2$, or in the case of the electron, $I_e = I_{be} + q_{be}\, d^2$, where the subscript *be* denotes the beta electron and d^2 is the average square distance the beta particle is from the rotation axis during one complete orbit.

I assumed the beta electron is a solid sphere, so its moment of charge is $I_{be} = {}^2/_5\, q_{be}\, r_{be}^2$. I determined the average distance squared that the beta particle was from the moment axis during its orbit by assuming it followed a circular orbit, and realizing that the equation of the orbit, if assumed in an x – y plane, is $x^2 + y^2 = r_e^2$, or $x^2 = r_e^2 - y^2$. This relationship made the average distance squared

$$d^2 = \frac{\int_0^{r_e} x^2 dy}{\int_0^{r_e} dy} = \frac{\int_0^{r_e} (r_e^2 - y^2) dy}{\int_0^{r_e} dy} = \frac{r_e^3 - \frac{1}{3} r_e^3}{r_e} = \tfrac{2}{3} r_e^2. \tag{18}$$

This made the product of the beta electron charge and its average distance squared from the moment axis during a complete orbit $q_{be}\, d^2 = {}^2/_3\, q_{be}\, r_e^2 = {}^2/_3\, q_e\, r_e^2$, since $q_{be} = q_e$. This is equal to the hollow-sphere electron moment of charge. Using it and the beta electron moment of charge, the actual moment of charge for the electron, $I_e = I_{be} + q_{be}\, d^2$, becomes $I_e = {}^2/_5\, q_{be}\, r_{be}^2 + {}^2/_3\, q_e\, r_e^2$, or

$$I_e = (\tfrac{3}{5} \frac{r_{be}^2}{r_e^2} + 1)(\tfrac{2}{3} q_e r_e^2). \tag{19}$$

I concluded that the expression in the first set of parenthesis in equation (19) corrects the hollow sphere approximation of the electron moment of charge that the Bohr magneton makes for the magnetic moment. If so, then

$$(\tfrac{3}{5}\frac{r_{be}^2}{r_e^2}+1)=1.00116, \quad (20)$$

or

$$r_{be}=0.04397\,r_e\,. \quad (21)$$

The classical radius of the electron is 2.82 x 10^{-15} m. Assuming it is the actual electron radius, the radius of the beta electron becomes

$$r_{be} = 1.24\ x\ 10^{-16}\ \text{m}. \quad (22)$$

This all implies that the beta electron goes into a high-frequency orbit with a radius about 23 times its radius when it is freed from a nucleon. This essentially creates a thin-shelled hollow sphere that I believe houses the neutrino that beta electron captures to become a free electron.

4.4 Neutron Model

My neutron model is a simple modification of the proton model. The deep inelastic scattering of the deuteron shows that the two nucleons in it look the same. It shows that the deuteron consists of particles that carry $^1/_{18}$ its mass, making all of the particles in the deuteron appear to be muons (see Section 2). Therefore, if one of the nucleons in the deuteron is a neutron, it looks almost exactly like a proton. It is made of a total of nine muons and antimuons. However, this creates a problem because a free neutron has no net charge. The simplest way I could get that by combining muon and antimuons was to have an equal number of each making up the neutron. The scattering showed that this is not the case.

Another way that I could create a neutron that looks almost like a proton was to add an electron to a proton. Adding an electron to a proton neutralizes its positive charge. However, the neutron mass is 1,838.68 times that of a free electron compared to 1,836.15 for the proton. The mass of the neutron is 2.5 free electron masses more than the proton. If I added a single electron to the proton, it would leave the neutron model 1.5 electron masses low. Adding two electrons would get me to within 0.5 electron masses of the measured neutron mass, but adding two electrons or an electron and a positron would give it a non-zero net charge again.

The only way that I could get close to the neutron mass and get its neutral charge was by adding an electron and an electron-positron pair to the proton. That gave the modified proton a zero net charge and a mass of about 1,839 electron masses, within 0.5 electron masses of the neutron mass. Adding the three particles to my proton model made my neutron model contain 920 electrons and 920 positrons, or 1,840 particles. When I apply the mass conversion factor of 0.99954 for beta electrons, my neutron model mass becomes 1,839.15 free electron masses.

My neutron model is still the four-muon, five-antimuon proton. The proton now just has three additional rogue particles in it. Eventually, it expels its three guests that turns it into a neutron through beta decay, and regains its true identity. Based on the beta decay, I placed those three particles all within just one of the proton's muons or antimuons in my neutron model. I did this because when a neutron decays, it emits a beta electron. It appears the energy that propels the extra beta electron out of the neutron comes from the annihilation of the extra electron-positron pair in the neutron. For this to happen, the three particles must be together.

The particles in the electron-positron pair eventually annihilate each other, producing 1.02 MeV of energy. This energy is what kicks the extra beta electron out of the neutron. However, during the decay, only 0.78 MeV of the 1.02 MeV from the annihilation appears as decay energy. The ejected beta electron captures the neutrino from a neutrino-antineutrino pair produced during the decay, to become a free electron. Then, the free electron and the remaining antineutrino fly off as decay products carrying a total of 0.78 MeV of energy, leaving a proton behind,

$$\begin{aligned} {}^{1}_{0}n &\rightarrow {}^{1}_{1}p \;+\; \beta^{-} + \;\gamma \;+\; 0.78\,MeV \\ &\rightarrow {}^{1}_{1}p \;+\; \beta^{-} + \;(\nu_e \;+\; \overline{\nu}_e) \;+\; 0.78\,MeV \\ &\rightarrow {}^{1}_{1}p \;+\; (\beta^{-} + \;\nu_e) \;+\; \overline{\nu}_e \;+\; 0.78\,MeV \\ &\rightarrow {}^{1}_{1}p \;+\; {}^{0}_{-1}e \;\;+\; \overline{\nu}_e \;\;+\; 0.78\,MeV. \end{aligned} \tag{23}$$

What happened to the other 0.24 MeV from the annihilation? I suspect that the emitted beta electron uses the remaining 0.24 MeV from the pair annihilation to free itself from the muon configuration. For this to happen, the three extra particles inside a proton that make it a neutron must all be in the same muon or antimuon.

The mass of the neutron is determined indirectly through mass-energy balances of various nuclear reactions such as the decay of the neutron or the absorption of a neutron by a proton to form a deuteron [30]. If the rogue beta electron is, indeed, held within the neutron by a 0.24 MeV potential; without knowing that, the energy to free it would not be accounted for in the mass-energy balance of the neutron. If that is the case, the steps in equation (23) are actually

$$\begin{aligned} {}^{1}_{0}n &\rightarrow {}^{1}_{0}n^{*} \;+\; 1.02\,MeV \\ &\rightarrow ({}^{1}_{0}n^{*} + \;0.24\,MeV) + \;0.78\,MeV \\ &\rightarrow {}^{1}_{1}p \;+\; \beta^{-} + \;\gamma \;+\; 0.78\,MeV \\ &\rightarrow {}^{1}_{1}p \;+\; \beta^{-} + \;(\nu_e \;+\; \overline{\nu}_e) \;+\; 0.78\,MeV \\ &\rightarrow {}^{1}_{1}p \;+\; (\beta^{-} + \;\nu_e) \;+\; \overline{\nu}_e \;+\; 0.78\,MeV \\ &\rightarrow {}^{1}_{1}p \;+\; {}^{0}_{-1}e \;\;+\; \overline{\nu}_e \;\;+\; 0.78\,MeV. \end{aligned} \tag{24}$$

In this sequence of events, the n^{*} is the neutron minus the electron-positron pair that annihilated creating the 1.02 MeV of energy. The remaining rouge beta electron is held in the neutron by 0.24 MeV. In the second step of equation (24), the beta electron acquires 0.24 MeV from the annihilation energy to free itself. By the third step of (24) the beta electron is free and the 472 eV-photon is created that will supply the neutrino the electron needs to become a free electron. This indicates that the neutron's mass is actually 0.24 MeV more than mass balances currently show.

A mass difference of 0.24 MeV is equivalent to 0.47 free electron masses. Recall that the mass of my alternative neutron model is 1,839.15 times the mass of a free electron, not the measured mass of 1,838.68 electron masses. If I add this mass that is not accounted for in the neutron mass determination to the currently reported measured mass, I get a new measured mass that is 1,838.68 + 0.47, or 1,839.15 times the mass of a free electron. This mass is now equal to my neutron model mass. It shows that the neutron is a proton plus two electrons and a positron.

5. Conclusions

I can draw at least three conclusions from my analyses. First, the data from *e-p* and *e-d* deep inelastic scattering experiments performed by SLAC and *e-p* experiments by HERA do support a simpler model of the proton than the quark-gluon model. I found that the SLAC data supports a proton made of nine particles which, based on their physical characteristics, appear to be muons and antimuons. I discovered that the HERA data appears to be that of deep inelastic scattering within the muons and antimuons making up the proton. It revealed that those muons and antimuons are each made of an average of 204 particles whose physical characteristics suggest that they are electrons and positrons.

Second, the proposed proton model is also more accommodating than the quark-gluon proton model. It provides a basis for explaining a variety of subatomic phenomena the quark-gluon model cannot explain. Its component muons and antimuons provide a source for the muons and antimuons observed during *e-p* deep inelastic scattering and in cosmic rays. Its component electrons and positrons provide a nuclear source for the particles emitted during beta decay. The model uses particle sharing between the muons and antimuons within the proton to bind them together. This is likely that the same mechanism that links nucleons together to form the nucleus of the atom. It revealed that the electrons inside the proton are slightly less massive than free electrons. This led to an alternative electron model where the free electron is an electron of the type found inside the proton (beta electron) coupled with a neutrino. This electron model makes the mass of the electron neutrino 236 eV, about 100 times more massive than it is currently thought to be. The electron model also appears to reveal why the Bohr magneton is only an approximation of the electron magnetic moment and how to correct it.

Third, the simplicity and transparency of the proposed model strongly suggest that the currently accepted proton model consisting of quarks and gluons is wrong. The proposed model shows that the proton can be modeled using particles, muons and electrons, which are observed routinely in nature, unlike quarks and gluons of the current model. It shows that when a proton shatters, the muons and antimuons that appear in the debris are likely the proton's components, as are the electrons and positrons that exit the nucleus during beta decay. The absence of quarks and gluons during those events should call into question whether they really exist.

All things considered, the most damning evidence against quarks being proton components may be the low-x, low-Q^2 data generated by JLAB that completes the SLAC proton and deuteron F_2 structure function curves (section 2.4). This data shows that the F_2 values in the low-x region of the curve were not lifted, so electrons were not scattering off quark-antiquark pairs. The data shows that the F_2 curve actually peaked at momentum fraction $x = {}^1/_9$ not $x = {}^1/_3$, indicating that the proton is made of nine particles, not three. Together, these findings essentially eliminate the sea quarks and the three valence quarks from contention as proton components.

I can make one final observation regarding my alternative model. It seems to give the visible universe an equal amount of matter and antimatter. Since positrons are the antimatter particles to electrons, if protons and neutrons are made of essentially the same number of each, then the universe contains about the same amount of antimatter as it does matter. In fact, in my model the proton has one unpaired positron in it. Since there is an electron for each proton in neutral atoms, then they contain an equal amount of matter and antimatter. This alternative proton model appears to eliminate the perceived matter-antimatter imbalance in the universe.

References

[1] A. Bodek, Nucl. Phys. B – Proc. Suppl. 139, 165 (2005).
[2] E.D. Bloom, *et al.*, Phys. Rev. Lett. 23, 930 (1969).
[3] J.S. Poucher, *et al.*, Phys. Rev. Lett. 32, 118 (1974).
[4] G. Miller, *et al.*, Phys. Rev. D 5 528 (1972).
[5] W.B. Atwood, *et al.*, Phys. Lett. 64B, 479 (1976).
[6] A. Bodek, *et al.*, Phys Rev D 20, 1471 (1973).
[7] T. Ahmed, *et al.* (H1 Collaboration), Nucl. Phys. B, 439, 471 (1995).
[8] J.D. Bjorken, Phys. Rev. 179 (1969) 1547.
[9] C.G. Callan and D.J. Gross, Phys. Rev. Lett. 22 156 (1969).
[10] M. Gell-Mann, Phys. Lett. 8 214 (1964).
[11] G. Zweig, An SU(3) model for strong interaction symmetry and its breaking II, CERN-8419-TH-412, (1964).
[12] M. Riordan, Science 256, 1287, (1992).
[13] R.P. Feynman, Science 183, 601 (1974).
[14] R.P. Feynman, Phys. Rev. Lett. 23, 1415 (1969).
[15] J.D. Bjorken and E.A. Paschos, Phys. Rev. 185, 1975 (1969).
[16] F. Halzen and A.D. Martin, *Quarks & Leptons: An introductory course in modern particle physics*, Chap. 9, John Wiley and Sons (1984).
[17] A. Bodek, *et al.*, Phys. Rev. Lett. 30, 1087 (1973).
[18] J. Kuti and V.F. Weisskopf, Phys. Rev. D 4, 3418 (1971).
[19] L.W. Whitlow, PhD. Thesis, Stanford University, SLAC- 357, Appendix E (1990).
[20] L.W. Whitlow, *et al*., Phys. Lett. B 250, 193 (1990).
[21] V. Tvaskis, et al., Phys. Rev. C 81, 055207, 305 (2010).
[22] M. Derrick, *et al.* (ZEUS Collaboration), Z. Phys. C 69, 607 (1996).
[23] J. Beringer *et al.* (Particle Data Group), Phys. Rev. D 86, 010001, 305 (2012).
[24] A. Aktas, *et al.* (H1 Collaboration), Phys. Lett. B 583, 28 (2004).
[25] C. Weinheimer, *et al.*, Phys. Lett. B 460, 219 (1999).
[26] V.M. Lobashev, *et al.*, Phys. Lett. B 460, 227 (1999).
[27] K. Assamagan, *et al.*, Phys. Rev. D 53, 6065 (1996).
[28] P.J. Mohr, *et al*., Rev. Mod. Phys. 80, 710 (2006).
[29] A.D. Polyanin and A.I. Chernoutsan, *A concise handbook of mathematics, physics, and engineering sciences*, 430, Chapman & Hall/CRC (2011).
[30] G.L. Greene, *et al.*, Phys. Rev. Lett. 56, 819 (1986).